

FORMATION FLIGHT STABILITY IN A GRAVITATIONAL FIELD

Nico Sneeuw, Mohammad A. Sharifi, and Hanspeter
Schaub



3rd International Symposium on Formation Flying

Noordwijk, The Netherlands

April 23–25, 2008

FORMATION FLIGHT STABILITY IN A GRAVITATIONAL FIELD

Nico Sneeuw¹, Mohammad A. Sharifi², and Hanspeter Schaub³

¹*Institute of Geodesy, Universität Stuttgart, Geschwister-Scholl-Str. 24D, D-70174 Stuttgart, Germany,
Email: sneeuw@gis.uni-stuttgart.de*

²*Surveying and Geomatics Engineering Dept., University college of Engineering, University of Tehran, Iran,
Email: sharifi@ut.ac.ir*

³*Aerospace and Engineering Sciences Department, University of Colorado, Boulder, CO 80309-0431, Email:
hanspeter.schaub@colorado.edu*

ABSTRACT

In this paper we investigate the boundedness and time evolution of four generic types of formation flights, GRACE, Cartwheel, Pendulum and LISA, due to gravitational perturbations. We start our analysis in a central field and step-wise add more complexity: first J_2 , then further zonals and finally a realistic gravitational field. The contribution of different gravitational components is investigated by analysis of the missions' relative motion. In particular the boundedness is quantified by the time behaviour or the intersatellite baseline. Also, the role of perigee precession is emphasized.

Key words: Formation flight; GRACE; Cartwheel; Pendulum ; LISA.

1. INTRODUCTION

With the launch of the Gravity Recovery And Climate Experiment (GRACE) mission an old dream of geodesists came true. It is the first realization of the concept of Satellite-to-Satellite Tracking (SST) in the low-low mode, i.e. the measurement of intersatellite baselinelength in a leader-follower configuration, which globally portrays the Earth's gravitational field with unprecedented resolution and accuracy [14].

The monthly GRACE solutions consistently exhibit typical erroneous North-South features [14]. Although this error behaviour is often associated with the ground-track of the near-polar GRACE satellites, it was argued by [12] that the inherent culprit is the non-isotropic SST observable. GRACE's K-band range-rate observable is sensitive in the along-track direction and carries no radial or cross-track information in the signal content. It is asserted that any observation geometry that could include radial and/or cross-track gravitational signal would enhance the

gravity signal and, hence, improve the gravity recovery capability. Note that aliasing behaviour, due to mass variations in the Earth system that are faster than the one-month GRACE sampling rate, will not be eliminated and will still produce North-South error features.

To support and quantify the above assertion [13] describes a gravity recovery experiment that makes use of the concept of formation flying. Four generic types of Low-Earth Formations (LEF) were simulated: a GRACE-type leader-follower configuration, a Cartwheel formation that performs a 2:1-relative ellipse in the orbital plane, a Pendulum mission and a LISA-type formation that performs circular relative motion including out-of-plane motion. The dynamics of such formations are easily understood in the framework of homogeneous Hill equations, cf. [12], although the implementation in a realistic gravity field requires careful attention to many fine details. All four LEF considered will have a typical baseline length of around 10 km. The names GRACE, Cartwheel Pendulum and LISA will be used in this paper as placeholders for these generic formations and should not be mistaken for the actual missions.

This paper is concerned with demonstrating the feasibility of such Formation Flying (FF) missions for gravity recovery purposes. The relative motion between satellites within a formation is highly correlated with the nature of the gravitational force of the main attracting body. Thus, mission stability, secular and periodic perturbation of the formation can be explained to a great extent by analyzing the gravitational perturbations.

In this study we therefore investigate the relative motion within a formation in different types of gravitational fields. We start with a central force field and gradually add gravitational complexity. The issue of boundedness within a central field is elementary and can be demonstrated analytically. The formation evolution in a J_2 -field and subsequently in a general zonal field can partially still be discussed an-

analytically, although we show some numerically integrated baseline evolutions, too. The development of the intersatellite baseline in a full gravitational field is analyzed by numerical integration over a period of one month.

2. RELATIVE MOTION IN THE CENTRAL FIELD

2.1. Hill equations

Let us adopt the following FF convention. All 4 formations consist of a chief satellite and a deputy satellites. We assume a local orbital reference frame (or Hill frame) with its origin in this chief satellite and oriented in along-track (x), cross-track or orbit-normal (y) and radial (z) direction. The relative motion of the deputy in the local orbital reference frame is described in general by [11]:

$$\ddot{x} + z\ddot{\theta} + 2\dot{z}\dot{\theta} - x\left(\dot{\theta}^2 - \frac{\mu}{r_c^3}\right) = a_x \quad (1a)$$

$$\ddot{y} + \frac{\mu}{r_c^3}y = a_y \quad (1b)$$

$$\ddot{z} - z\left(\dot{\theta}^2 + 2\frac{\mu}{r_c^3}\right) - x\ddot{\theta} - 2\dot{x}\dot{\theta} = a_z \quad (1c)$$

where μ is the gravitational constant and (a_x, a_y, a_z) are non-Keplerian forces acting on the deputy satellite. They could be due to atmospheric drag, Earth oblateness effects or control thrusters.

Here we consider only formations where the chief motion is essentially circular. In this case the chief rate $\dot{\theta}$ is constant and equal to the mean orbit rate $n = \sqrt{\mu/r_c^3}$. The equations of motion simplify to the well-known linearized Hill Equations (HE) [5], see also [4]:

$$\ddot{x} + 2n\dot{z} = a_x \quad (2a)$$

$$\ddot{y} + n^2y = a_y \quad (2b)$$

$$\ddot{z} - 2n\dot{x} - 3n^2z = a_z \quad (2c)$$

Equation (2) has been used extensively in spacecraft formation flying mission analysis and control research. They are reasonable as long as (x, y, z) are small compared to the chief orbital radius and the chief motion is essentially circular.

Since they are linear, the HE can be solved analytically. Assuming no perturbations or thrusting is present ($a_x = a_y = a_z = 0$), all possible deputy relative motions can be expressed in the following closed form [11]:

$$x(t) = -2A_0 \sin(nt + \alpha) - \frac{3}{2}ntz_{\text{off}} + x_{\text{off}} \quad (3a)$$

$$y(t) = B_0 \cos(nt + \beta) \quad (3b)$$

$$z(t) = A_0 \cos(nt + \alpha) + z_{\text{off}} \quad (3c)$$

Note that the out-of-plane motion is decoupled from the in-plane motion. The integration constants can be expressed in terms of initial conditions through:

$$A_0 = \frac{1}{n} \sqrt{\dot{z}_0^2 + (2\dot{x}_0 + 3nz_0)^2} \quad (4a)$$

$$B_0 = \frac{1}{n} \sqrt{\dot{y}_0^2 + (ny_0)^2} \quad (4b)$$

$$\alpha = \arctan\left(\frac{\dot{z}_0}{3nz_0 + 2\dot{x}_0}\right) \quad (4c)$$

$$\beta = \arctan\left(\frac{-\dot{y}_0}{ny_0}\right) \quad (4d)$$

$$z_{\text{off}} = \frac{2}{n}(\dot{x}_0 + 2nz_0) \quad (4e)$$

$$x_{\text{off}} = x_0 - \frac{2\dot{z}_0}{n} \quad (4f)$$

The solution of the homogeneous HE allows the analysis of arbitrary formation flight motion in terms of the initial Cartesian state conditions used in (4).

2.2. Condition of bounded relative motion

For the relative motion to be bounded, we must require the drift term to vanish, i.e. $z_{\text{off}} = 0$ for all missions. Therefore,

$$\dot{x}_0 = -2nz_0 \quad (5)$$

Fulfilling this condition also removes the constant offset in the radial component. Similarly one can derive the equal phase angle condition $\alpha = \beta$ as,

$$y_0 \dot{z}_0 - \dot{y}_0 z_0 = 0. \quad (6)$$

Eventually, setting $x_{\text{off}} = 0$ leads to a formation flight with periodic along-track component with no secular drift.

Equations (5) and (6) give the necessary conditions for a bounded motion in a central gravity field. Alternatively, [9] has derived the solution of the homogeneous HE in terms of the classical Keplerian orbit element differences as

$$x(t) = -2a\Delta e \sin(\nu \pm \pi - \Delta\omega) + a(\Delta u_0 + \Delta\Omega \cos I) - \frac{3}{2}nt\Delta a \quad (7a)$$

$$y(t) = a \sqrt{\Delta I^2 + \Delta\Omega^2 \sin^2 I} \cos(u - u_y) \quad (7b)$$

$$z(t) = a\Delta e \cos(\nu \pm \pi - \Delta\omega) + \Delta a \quad (7c)$$

with

$$u_y = \arctan\left(\frac{\Delta I}{-\Delta\Omega \sin I}\right) \quad (8)$$

Analogously, the boundedness condition can also be expressed using the differential classical Keplerian orbit elements.

$$\Delta a = 0. \quad (9)$$

An identical orbit period both for the chief and deputy satellites is a direct consequence of this condition. Furthermore, the constant bias of the radial motion also vanishes. Note that while the condition in equation (5) is a linear approximation result, the equal orbit energy condition in equation (9) is the full solution for the central gravity field model.

The equal phase angle condition is recast using classical orbit element differences into

$$\tan(\omega + \Delta\omega \pm \pi) = \frac{\Delta I}{-\Delta\Omega \sin I} \quad (10)$$

Eventually, fulfilling

$$\Delta u_0 + \Delta\Omega \cos I = n(2\pi), \quad (11)$$

removes the constant term of the along-track component.

Independent from the formation design, the bounded motion condition (5) or (9) should be satisfied. However, the other conditions can be used to design different flying formations.

2.3. Formation design

The four generic FF types are characterized by the following descriptions:

- GRACE is a pure along-track formation. All periodic terms are zero and the variable x_{off} determines the baseline length.

$$x(t) = \rho \quad (12a)$$

$$y(t) = 0 \quad (12b)$$

$$z(t) = 0 \quad (12c)$$

which ρ is the baseline length between the spacecrafts.

- The pendulum scenario also has a constant along-track term x_{off} , but additionally a non-zero cross-track amplitude B_0 . The relative motion takes place in the xy -plane, i.e. the local horizontal plane. The intersatellite baseline is variable. Only its component in the along-track direction (ρ_x) is constant whereas the cross-track component ρ_y oscillates at twice the orbital frequency 1CPR.

$$x(t) = \rho_x \quad (13a)$$

$$y(t) = \rho_y \cos(nt + \beta) \quad (13b)$$

$$z(t) = 0 \quad (13c)$$

It is clear that the phase shift in the cross-track component can be realized if the satellites orbit the Earth in orbital planes with different inclinations. The relationship between the cross-track phase shift and the differential orbital elements is explicitly expressed in (8). A non-zero value for the differential inclination yields a cross-track phase shift.

- The Cartwheel configuration has a non-zero A_0 value. Without cross-track motion ($B_0 = 0$) this results in an in-plane elliptical relative motion [8]. The maximum along-track separation is twice as large as the maximum radial separation. Hence a 2:1 relative ellipse

$$\frac{x^2}{4\rho_z^2} + \frac{z^2}{\rho_z^2} = 1, \quad (14)$$

where ρ_z is the maximum radial separation.

- The LISA-type mission achieves a circular relative motion by setting $B_0 = \sqrt{3}A_0$ and matching the phases α and β . Within the approximation of the HE, the baseline is constant. Projection of the circular motion on the xy and xz forms two ellipses whereas the relative motion in the yz plane is a purely linear motion.

$$\frac{x^2}{\rho^2} + \frac{y^2}{\frac{3\rho^2}{4}} = 1 \quad (15a)$$

$$\frac{x^2}{\rho^2} + \frac{y^2}{\frac{\rho^2}{4}} = 1 \quad (15b)$$

$$y = \sqrt{3}z \quad (15c)$$

Figure 1 shows the relative motion of the aforementioned formation types. All the three components are constant for the GRACE type mission whereas the Pendulum has a constant along-track and a variable cross-track component. The Cartwheel's components vary both in the along-track and radial directions. The LISA type mission has variable components in all three directions.

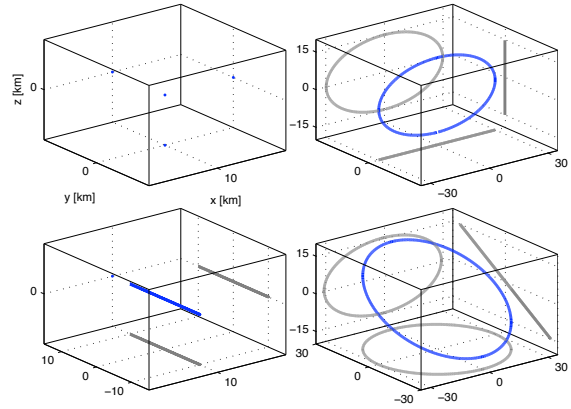


Figure 1. Relative motion of four formation types in the Hill frame: GRACE (top left), Cartwheel (top right), Pendulum (lower left) and LISA (lower right).

The necessary condition for achieving these configurations and the corresponding differential elements in the Hill frame are summarized in table 1. These differential elements can be converted to inertial orbital

Table 1. Initial conditions and state vectors of different formation types.

| formation | initial conditions | initial position (ρ_0) | initial velocity ($\dot{\rho}_0$) |
|-----------|---|--|---|
| GRACE | $A_0 = B_0 = z_{\text{off}} = 0$ | $(\rho, 0, 0)$ | $(0, 0, 0)$ |
| Pendulum | $A_0 = z_{\text{off}} = 0$ | $(\rho_x, \rho_y \cos \beta, 0)$ | $(0, -n\rho_y \sin \beta, 0)$ |
| Cartwheel | $B_0 = x_{\text{off}} = z_{\text{off}} = 0$ | $(\pm 2\sqrt{4a^2e^2 - z_0^2}, 0, z_0 \leq 2ae)$ | $(-2nz_0, 0, \pm n\sqrt{4a^2e^2 - z_0^2})$ |
| LISA | $x_{\text{off}} = z_{\text{off}} = 0; \alpha = \beta$ $B_0 = \sqrt{3}A_0 = \sqrt{3}\rho/2$ | $(\pm\sqrt{\rho^2 - 4z_0^2}, \pm\sqrt{3}z_0, z_0 \leq \rho/2)$ | $(-2nz_0, \pm\sqrt{3}n\sqrt{\rho^2/4 - z_0^2}, \pm n\sqrt{\rho^2/4 - z_0^2})$ |

elements for integration purposes [1]. In table 1, relative position and velocity vectors are expressed in terms of the chief satellite's Kepler elements (a, e, u) and the baseline length ρ . The latter two configurations are defined by setting the free parameter (z_0) .

3. RELATIVE MOTION IN J_2 FIELD

The homogeneous HE are a helpful tool for first order formation design. However, the solution in (3) is no longer valid if the chief motion is not circular. Even small amounts of eccentricity can produce modelling errors comparable to those produced by J_2 gravitational perturbations or atmospheric drag. Moreover, the analytical relative motion solutions in equation (3) have been derived based on the Keplerian motion. In reality, satellites are perturbed by different disturbing forces. Among them, the Earth flattening dominantly affects LEO satellites motion in such a way that the aforementioned constraints are not sufficient to guarantee the desired relative orbit geometry. Therefore, formation flight design would be more realistic if we take J_2 -field perturbation into account.

In general, the gravitational potential for an arbitrary point with spherical coordinates (r, θ, λ) can be represented as:

$$V(r, \theta, \lambda) = \frac{\mu}{r} + R(r, \theta, \lambda, \bar{C}_{lm}, \bar{S}_{lm}), \quad (16)$$

with $\mu = GM_e$, the universal gravitational constant times mass of the Earth. The contribution of the spherical harmonic coefficients \bar{C}_{lm} and \bar{S}_{lm} is represented by the disturbing function R . They lead to time variable orbital elements known as *osculating elements*. The equations of motion, describing the time evolution of these elements, are *Lagrange's Planetary Equations* (LPE), cf. [7].

The disturbing potential R causes *periodic and secular* perturbations on the orbital elements. In particular, the degree 2 zonal harmonic J_2 , corresponding to the Earth's flattening, causes strong drift effects, long-term oscillations and short-term oscillations at twice the orbital frequency [3].

For purposes of formation keeping at least the secular relative drift between the satellites should be can-

celled. For this purpose the cyclic short- and long-period terms are averaged out of the J_2 disturbing function:

$$\bar{R}_2(a, e, I) = \frac{\epsilon(a, e)\eta\mu}{2a} \left(\frac{1}{3} - \frac{1}{2} \sin^2 I \right) \quad (17)$$

with $\epsilon(a, e) = 3J_2a_e^2/a^2\eta^4$ and the eccentricity measure $\eta = \sqrt{1 - e^2}$. Inserting (17) into the LPE gives expressions for the first-order secular perturbation:

$$\dot{a} = \dot{e} = \dot{I} = 0, \quad (18a)$$

$$\dot{\Omega} = -\frac{\epsilon(a, e)}{2} n \cos I, \quad (18b)$$

$$\dot{\omega} = \frac{\epsilon(a, e)}{4} n(5 \cos^2 I - 1), \quad (18c)$$

$$\dot{M} = n \left[1 + \frac{\epsilon(a, e)}{4} \eta(3 \cos^2 I - 1) \right]. \quad (18d)$$

with the chief mean motion being $n = \sqrt{\mu/a^3}$. First, the secular rates are independent from Ω , ω and M . Consequently, they can be selected freely to form a desired formation. Second, the right ascension of the ascending node Ω , the argument of perigee ω and the mean anomaly M all experience drift. Therefore, a cluster of satellites retains its relative geometry if the drifts of the satellites are identical. Reference [10] refers to such relative orbits as J_2 -invariant. For simplicity, consider a cluster with two satellites whose *mean Keplerian elements* are given by $(a_1, e_1, I_1, \Omega_1, \omega_1, M_1)$ and $(a_2, e_2, I_2, \Omega_2, \omega_2, M_2)$. A formation will not experience secular drift in a J_2 gravity field if the following constraints are fulfilled:

$$\begin{cases} \Delta\dot{\Omega}_{12} = \dot{\Omega}_2 - \dot{\Omega}_1 = 0 \\ \Delta\dot{\omega}_{12} = \dot{\omega}_2 - \dot{\omega}_1 = 0 \\ \Delta\dot{M}_{12} = \dot{M}_2 - \dot{M}_1 = 0 \end{cases} \quad (19)$$

The conditions define a nonlinear system of 3 equations in $a_1, a_2, e_1, e_2, I_1, I_2$. In formation design one usually fixes the orbital parameters of one satellite. The aim is to find the differential elements $\Delta a, \Delta e$ and ΔI that realize a bounded formation. Hence,

$$\begin{cases} \Delta\dot{\Omega}_{12}(\Delta a, \Delta e, \Delta I) = 0 \\ \Delta\dot{\omega}_{12}(\Delta a, \Delta e, \Delta I) = 0 \\ \Delta\dot{M}_{12}(\Delta a, \Delta e, \Delta I) = 0 \end{cases} \quad (20)$$

Since the differential elements $\Delta a, \Delta e$ and ΔI are usually small, the nonlinear equations (20) can be

replaced by a linearized system of equations

$$\mathbf{J}_{a,e,I}^{\dot{\Omega},\dot{\omega},\dot{M}}(a_1, e_1, I_1)\mathbf{x} = \mathbf{0}. \quad (21)$$

with $\mathbf{x} = [\Delta a, \Delta e, \Delta I]^T$. The Jacobian \mathbf{J} contains the partial derivatives of the drift toward the metric Kepler elements a, e, I , evaluated in the master satellite. The linear system (21) is a *homogeneous* system. If $\text{rank } \mathbf{J} = 3$ it will have the trivial solution only. Otherwise the system has many non-trivial solutions. Solving all three conditions in equation (21) leads to satellite clusters with very large separation distances. Instead, it is common to only solve a sub-set of conditions. For example the original J_2 -invariant relative motion conditions require that $\Delta\dot{\Omega}_{12} = 0$ and $\Delta\dot{\omega}_{12} + \Delta\dot{M}_{12} = 0$ is true to first order.

4. ZONAL GRAVITATIONAL FIELD

4.1. Secular perturbations

Although the Earth's flattening, represented by J_2 , is the dominant gravitational perturbation, other spherical harmonic components give rise to perturbations, too. In this section we consider the zonal field, i.e. that part of the gravitational field that does not depend on longitude. Such an axi-symmetric gravitational field is expressed as:

$$V(r, \theta) = \frac{\mu}{r} \left[1 - \sum_{n=2}^N \left(\frac{R}{r} \right)^n \bar{J}_n \bar{P}_n(\sin \theta) \right]. \quad (22)$$

Equivalently the disturbing force is

$$R_z(r, \theta, \bar{C}_{n0}) = -\frac{\mu}{r} \sum_{n=2}^N \left(\frac{R}{r} \right)^n \bar{J}_n \bar{P}_n(\sin \theta) \quad (23)$$

where \bar{P}_{n0} are the Legendre polynomials of degree n , The J_n are the zonal coefficients, which can also be expressed as $J_n = -C_{n,0}$, i.e. as non-normalized spherical harmonic coefficients of order 0.

Orbits of satellites around an axi-symmetric Earth are subject both to secular and periodic perturbations [2]. Similar to the J_2 -field perturbation, the secular variations of the orbit elements caused by the higher zonal harmonics can be derived from the LPE. Metric orbital elements (a, e and I) experience no secular variations, e.g. [2, 15]:

$$\dot{a}_z = \dot{e}_z = \dot{I}_z = 0. \quad (24)$$

Therefore, satellite orbits around an Earth with axially symmetric mass distribution are *size-shape stable*¹.

¹An orbit is called *size-shape stable* if its semi-major axis and eccentricity are constant on average [6]

Similar to the J_2 scenario, the angular elements (Ω, ω and M) do experience secular variations by the higher zonal harmonics. However, the secular perturbations in these elements are induced only by *even* zonal harmonics [7]. Reference [15] derives such perturbations by means of zero-degree Hansen coefficients. The rate of secular perturbations are only functions of the metric elements a, e and I .

$$\dot{\Omega}_{sz} = \dot{\Omega} + \delta\dot{\Omega}(a, e, I) \quad (25a)$$

$$\dot{\omega}_{sz} = \dot{\omega} + \delta\dot{\omega}(a, e, I) \quad (25b)$$

$$\dot{M}_{sz} = \dot{M} + \delta\dot{M}(a, e, I) \quad (25c)$$

which says that the secular rates, due to the general zonal gravity field, is composed of the J_2 secular rate (first term at right side) and a residual part from higher degree even zonal terms. For example, a LEO satellite with orbital elements $\{a, e, I, \Omega, \omega\} = \{6768 \text{ km}, 0.00007, 89.5^\circ, 0, 0\}$ is considered. Table 2 provides its secular rates for the gravitational field up to degree 6. As can be expected from the numer-

Table 2. Secular perturbation due to J_2 and J_2 - J_6 .

| Element | J_2 | $J_2 + J_4 + J_6$ |
|----------------|------------------|-------------------|
| $\dot{\Omega}$ | -0.0706[deg/day] | -0.0709[deg/day] |
| $\dot{\omega}$ | -4.0463 | -4.0578 |
| \dot{M} | -4.0469 | -3.9880 |

ical dominance of J_2 , the residual effect of the higher degree terms is moderate.

In the general zonal field the satellites within a formation experience identical secular variations in their angular elements as long as they have identical metric elements. Therefore, the conclusions from the previous section apply here as well. A formation that is drift-free in a J_2 field will be drift-free in an axially symmetric gravitational field, too.

4.2. Periodic perturbations

As discussed in section 3, the expressions for secular perturbations are achieved through averaging the cyclic terms in the disturbing functions. Thus, in reality non-secular variations will occur in all elements due to all zonal harmonics [2]. Such periodic variations of orbital elements can be formulated in terms of zero-order Hansen coefficients [15]. The general form of the expression for the long-periodic variations is

$$\dot{k}_{pz} = \dot{k}_{p2}(a, e, I, \omega) + \delta\dot{k}(a, e, I, \omega) \quad (26)$$

in which k can denote any of the Keplerian elements $\{a, e, I, \Omega, \omega\}$. The pz subscript stands for periodic variations produced by zonal harmonics whereas p2 represents the J_2 -field periodic perturbation. They

are decomposed into the second and higher zonal harmonics perturbations. Perturbations induced by second and higher degree zonals are functions of a , e , I and ω . In contrast to the previous statement about secular zonal perturbations, the satellites in a formation with identical metric elements are subject to *different* periodic variations.

To summarize these analytical findings: a formation's evolution will be bounded—in the sense that all differential secular motion is zero—as long as the individual satellites have identical Keplerian elements a , e and I . At the same time a differential perigee angle $\delta\omega$ will give rise to a differential (long) periodical motion, despite the identical metric elements. Consequently, the intersatellite baseline will show long period cyclic motion, too.

One interaction between secular and periodic evolution within the formation arises from perigee precession. The line of apsides continuously rotates due to the Earth's flattening. Thus, the satellites in a formation display different time-dependent long-periodic perturbations even if they have identical metric elements.

As a representative example, let us consider the Cartwheel type formation with the following differential elements:

$$\Delta a = \Delta e = \Delta I = \Delta \Omega = 0, \quad (27a)$$

$$\Delta \omega = \Delta M = \pi. \quad (27b)$$

The chief satellite's Keplerian elements are identical to the given values above Table 2. The long-term cyclic variations of the formation's differential orbital elements for a complete revolution of perigee are analyzed in a $J_2 + J_4$ gravitational field (by analytical means). The results are shown in Figures 2–6 as a function of the argument of perigee and compared to the corresponding variations in a J_2 field.

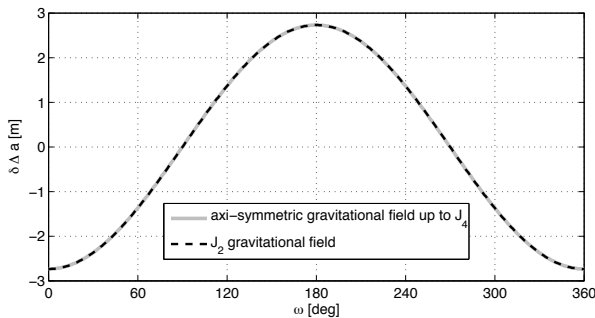


Figure 2. $\delta\Delta a$ long-periodic variation.

Despite the vanishing secular perturbations, long period variations do change the semi-major axes. The variations in a $J_2 + J_4$ field are equal to those in a J_2 field. The maximum deviation of the semi-major axes amounts to a few meters at 400 km altitude.

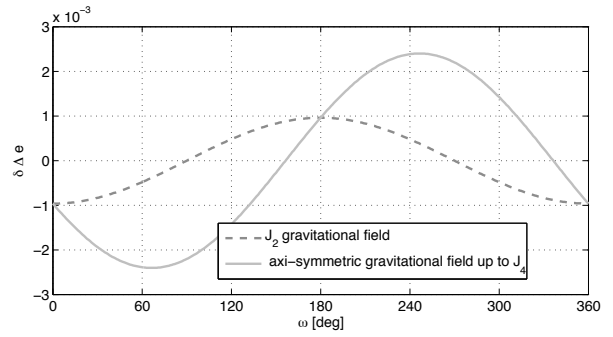


Figure 3. $\delta\Delta e$ long-periodic variation.

Also the differential eccentricity will undergo long-period variation as the apsidal line rotates. Different patterns are observed for J_2 and $J_2 + J_4$ fields.

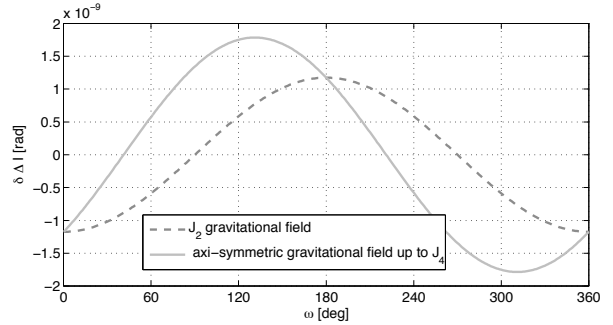


Figure 4. $\delta\Delta i$ long-periodic variation.

A similar comparison is shown for differential inclination behaviours. It is differently influenced by different zonal harmonics. Deviations of differential inclination from the nominal difference are mapped into the cross-track component.

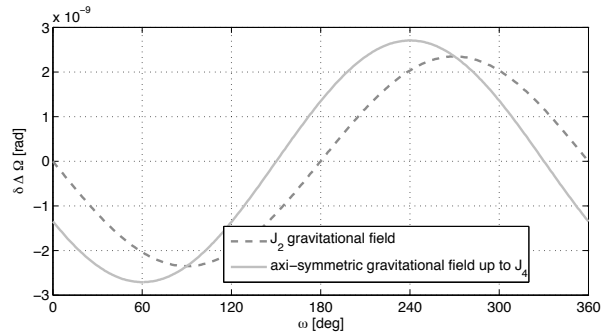


Figure 5. $\delta\Delta\Omega$ long-periodic variation.

Differential right-ascension is similarly affected by the zonal harmonics. The size of its deviation is about the variations of differential inclination.

The differential argument of perigee is significantly perturbed by the higher zonal harmonics. Its devia-

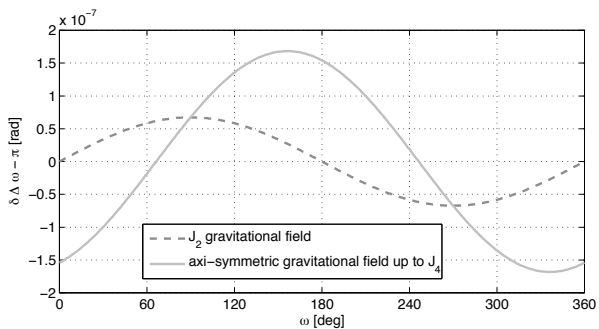


Figure 6. $\delta\Delta\omega$ long-periodic variation.

tions is nearly two orders of magnitude greater than the variations in ΔI and $\Delta\Omega$.

5. FULL GRAVITATIONAL FIELD

Beyond the zonal field, the real Earth gravity field is comprised of a full spectrum of spherical harmonic components. Without writing down the corresponding force function in terms of spherical harmonics, we consider here the *longitude-dependent* gravitational forces leads to

$$R(r, \theta, \lambda) = R_z(r, \theta) + R_{t,s}(r, \theta, \lambda) \quad (28)$$

in which the subscript t denotes *tesseral* and s denotes *sectorial* harmonics. The *tesseral*, *sectorial* or *longitude-dependent* component $R_{t,s}$ of the Earth's disturbing forces will additionally perturb the satellite orbit. Except for cases of resonance, they impose no secular perturbations.

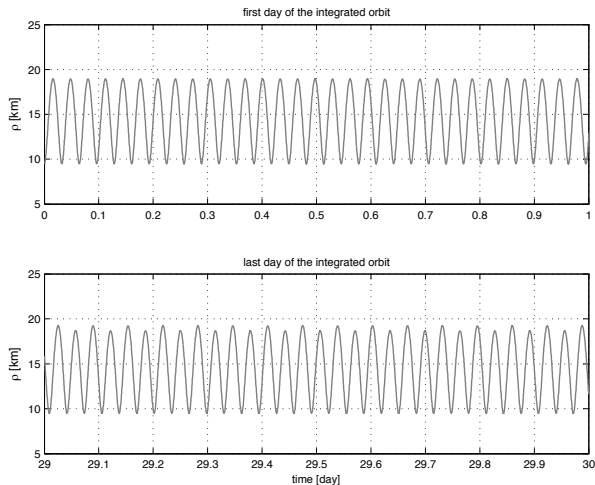


Figure 7. Cartwheel intersatellite distance in a J_2 field.

Reference [7] derived analytical expressions for perturbations of orbital elements due to given harmonics

\bar{C}_{nm} or \bar{S}_{nm} . Alternatively, [13] employed numerical integration to show the effect of the low-degree tesseral harmonics. The presence of the tesseral harmonics causes periodic variations on the intersatellite distance of all the formations (GRACE, Cartwheel, Pendulum and LISA).

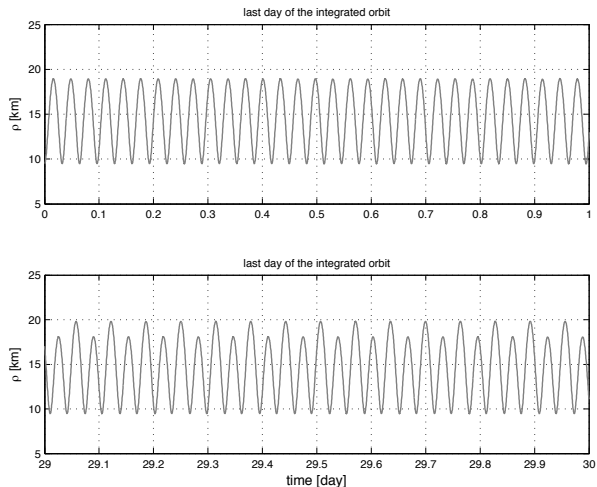


Figure 8. Cartwheel intersatellite distance in a full degree-2 field.

Figures 7 and 8 are the result of such a numerical integration of a Cartwheel type formation (relative ellipse about 10:20 km) over a 30-day period. The top panel of figure 7 shows that the baseline oscillates in the 1:2 ratio in a very stable way during the first day. After 30 days, the baseline oscillation is not in a 1:2 ratio anymore. Figure 8 demonstrates that in a full gravity field up to degree 2, including the non-zonal terms, this behaviour becomes even worse.

Simulations for the generic formation types GRACE, Pendulum and LISA show similar behaviour. The boundedness of formation evolution is mostly decided by the J_2 secular perturbations. But even if a formation is designed under the boundedness conditions higher harmonics will still cause periodic perturbations on the intersatellite distance.

As a last example, figure 9 shows what happens to the baseline in a low-Earth LISA formation due to the full gravity field. The orbits were integrated again over a 30-day period in order to capture the effects of perigee precession. The top panel shows a nearly constant intersatellite distance during the first day, which is expected for the circular relative LISA motion. After 30 days (bottom panel) the baseline wildly fluctuates, i.e. the relative circle does not exist anymore. This effect, mostly due to secular rotation of the apsidal line, is clearly demonstrated in the Hill frame, figure 10, particularly the top left panel.

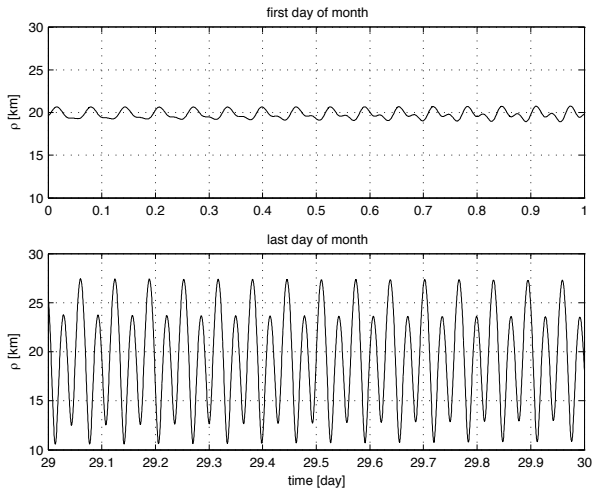


Figure 9. LISA intersatellite distance in a full gravity field.

6. CONCLUSIONS

By a stepwise increase in complexity of the gravity field, we analyzed the boundedness and more general behaviour of formation flights. The dominance of the Earth-flattening in the perturbation spectrum requires certain boundedness conditions. Identical metric elements lead to a bounded motion formation in a higher degree axi-symmetric gravitational field. Although the secular evolution can be kept in check, periodic effects will remain.

The perigee precession due to J_2 (and higher even zonals) is of particular concern as it induces long period effects to all Keplerian elements and, hence, deform the formation shape and the intersatellite distance itself. Higher spherical harmonic terms cause further periodic perturbations, mostly short term.

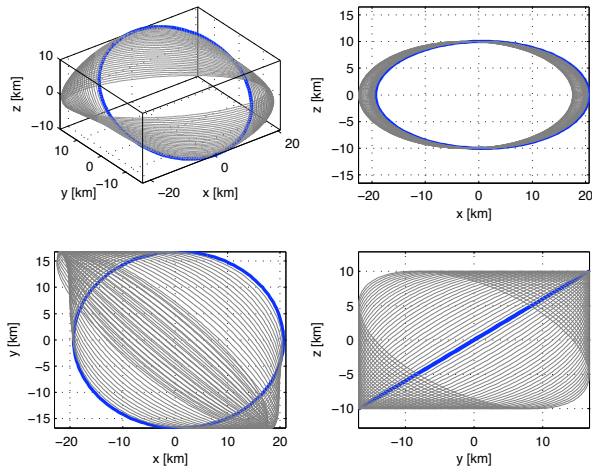


Figure 10. LISA relative motion in a full gravity field, viewed in the local orbital reference frame.

REFERENCES

- [1] K.T. Alfriend, H. Schaub, and D.W. Gim. Gravitational perturbations, nonlinearity and circular orbit assumption effects on formation flying control strategies. In *the Annual AAS Rocky Mountain Conference*, page 139158, Breckenridge, CO, February 2000.
- [2] L. Blitzer. Handbook of orbital perturbations. Technical report, university of Arizona, 1975.
- [3] Michel Capderou. *Satellites orbits and missions*. Springer, 2005.
- [4] W.H. Clohessy and R.S. Wiltshire. Terminal guidance system for satellite rendezvous. *Journal of the Aerospace Sciences*, 27:653–658, 1960.
- [5] G.W. Hill. Researches in the lunar theory. *Am. Journal of Math.*, 1:5–26,129–147,245–260, 1878.
- [6] W. Hu and D.J. Scheeres. Numerical determination of stability regions for orbital motion in uniformly rotating second degree and order gravity fields. *Planetary and Space Science*, 52:685–692, 2004.
- [7] W. M. Kaula. *Theory of satellite geodesy: Applications of satellites to geodesy*. Waltham, Mass.: Blaisdell, 1966.
- [8] D. Massonnet. The interferometric cartwheel: a constellation of passive satellite to produce radar images to be coherently combined. *Int. J. Remote Sensing*, 22:2413–2430, 2001.
- [9] H. Schaub. Relative orbit geometry through classical orbit element differences. *Journal of Guidance, Control and Dynamics*, 27(5):839–848, Sept.–Oct. 2004.
- [10] H. Schaub and K.T. Alfriend. J_2 invariant relative orbits for spacecraft formations. *Celestial Mechanics and Dynamical Astronomy*, 79(2):77–95, 2001.
- [11] H. Schaub and J. L. Junkins. *Analytical mechanics of space systems*. AIAA education series, Reston VA, 2003.
- [12] N. Sneeuw and H. Schaub. Satellite clusters for future gravity field missions. In C. Jekeli, L. Bastos, and J. Fernandes, editors, *Gravity, Geoid and space missions*, volume 129 of *IAG Symposia*, pages 12–17. IAG, Springer, 2005.
- [13] N. Sneeuw, M. A. Sharifi, and W. Keller. Gravity recovery from formation flight missions. In P.L. Xu, J.N. Liu, and A. Dermanis, editors, *Theoretical and Computational Geodesy: Challenge and Role of Modern Geodesy*, volume 132 of *IAG*. Springer, 2008.
- [14] B.D. Tapley, S. Bettadpur, J.C. Ries, P.F. Thompson, and M.M. Watkins. GRACE measurements of mass variability in the earth system. *Science*, 305:503–505, 2004.
- [15] B. Zafropoulos. The motion of a satellite in an axi-symmetric gravitational field. *Astrophysics and space science*, 139:111–128, 1987.